

## OPTIMIZATION OF CONTROL FACTORS INFLUENCING THE WEAR BEHAVIOUR OF AA7075/WC COMPOSITE

Irshad ALAM<sup>1</sup>, Nilamber Kumar SINGH<sup>2</sup>

*After conducting wear tests on a pin-on-disc machine, the control factors like sliding distance (500-1500 m), applied load (20-40 N) and sliding speed (1-3 m/s) are optimized (Taguchi method) for minimum wear loss in the developed (stir casting process) aluminium matrix composite (AA7075/2 wt.% WC). Elemental composition of the composite is identified and a uniform dispersion of the tungsten carbide (WC) reinforcement in the lightweight aluminium alloy (AA7075) matrix is ensured by EDX analysis. Optical microscope is used to study the worn-out surfaces. Vicker microhardness, density and porosity are determined. Also, the variation in friction coefficient with time under the influence of above parameters are investigated.*

**Keywords:** AA7075, WC, stir casting process, wear and Taguchi method.

### 1. Introduction

Owing to the high strength-to-mass ratio, stiffness, resistance to wear and corrosion, aluminum matrix composites (AMCs) are in demand for engineering applications such as aerospace, automotive and military sectors [1-4]. Several researchers [5-9] studied the wear characteristics of these AMCs based on its reinforcing materials like silicon carbide (SiC), alumina (Al<sub>2</sub>O<sub>3</sub>), barium carbide (B<sub>4</sub>C), titanium oxide (TiO<sub>2</sub>), carbon nanotubes (CNTs) etc. It is observed that the control parameters (sliding distance, applied load, sliding speed) affect the wear properties differently and therefore, optimization of these factors is needed to select more wear resistant composite involving those reinforcing materials for engineering structures [10-13]. Researches [14-16] are also available for optimization of the above control parameters to obtain high performance composites using Taguchi approach which improves the quality of products and processes by making them more robust. However, studies on the behaviour of AA7075/WC composite are rarely available in literature. Therefore, the aim of the paper is to develop the composite AA7075/2 wt.% WC using stir casting process and examine its wear characteristics. The control parameters (sliding distance,

---

<sup>1</sup>Res. Scho., National Institute of Technology Patna, India, e-mail: irshad.me@mitmuzaffarpur.org

<sup>2</sup>Assoc. Professor, National Institute of Technology Patna, India, e-mail: nilambersingh@nitp.ac.in

applied load and sliding speed) are optimized for maximum resistance to wear of the composite AA7075/WC using Taguchi method.

## 2. Experimental Procedure

### 2.1 Development of Composites

The composite, AA7075/2 wt.% WC is prepared by stir casting process (Fig. 1) where, the aluminium alloy AA7075 (Table 1) in the form of small pieces of rod is melted into liquid form at 800<sup>0</sup>C in an electric furnace (Fig. 1a) and impurities are removed. Then, the tungsten carbide (WC) powder (Table 2) as reinforcement is preheated to 300<sup>0</sup>C in preheat chamber of stir casting setup to remove its moisture and enhance the wettability of WC with molten metal. The preheated, 2 wt.% of WC reinforcement i.e. 10 grams, (selected based on prior studies [17,18]) is gradually added into the vortex of the molten melt (490 gram) created by the stirrer rotating at 300 rpm for 5 minutes. After adding the reinforcement, the mixing is continued further for 10 minutes with the stainless-steel stirrer at 300 rpm. This mixture is then casted in a preheated cast iron mould (Fig. 1b and Fig. 1c) and left for 60 minutes for cooling down in air. The prepared casting (Fig. 1d) is removed from the mould and finished as test samples (Fig. 1e).

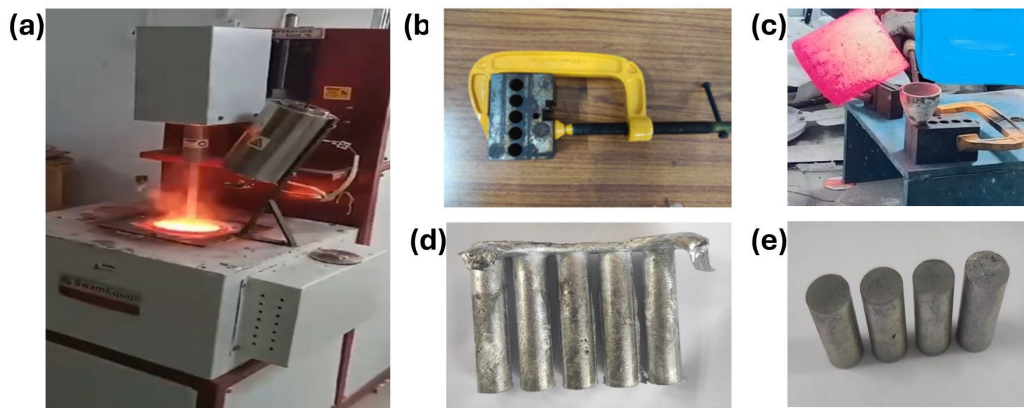


Fig. 1. Stir casting process (a) electric furnace (b) mould (c) mixture pouring in mould (d) casted samples and (e) test samples.

Table 1

Chemical Composition of AA7075 in weight%

Si	Cu	Fe	Zn	Mg	Su	Ti	Pb	Mn	Cr	Bi	Al
0.346	1.846	0.308	6.323	2.346	0.010	0.002	0.007	0.179	0.246	0.002	89.385

Table 2

Technical Data of Tungsten Carbide

Molecular Formula	Molecular Weight	Melting Point	Boiling Point	Density	APS	Purity	Color	Form
WC	195.85 g/mol	2785 - 2830°C	6000 °C	15.6 g/cm <sup>3</sup>	10-20 µm	99%	Black/Grey	Powder

## 2.2 Density

Theoretical and experimental/actual densities are required to assess the quality, composition, and structural integrity of a material. Porosity in the material is determined using these two densities.

*Theoretical density by 'rule of mixture'*: Equation (1) is used to calculate this density ( $\rho_{th}$ ) as 2.857 gm/cc. Density of the matrix (AA7075) is,  $\rho_m = 2.81$  gm/cc and that of the reinforcement (WC) is  $\rho_r = 15.6$  gm/cc, whereas, mass fraction of the matrix is,  $M_m = 0.98$  and that of the reinforcement is,  $M_r = 0.02$ .

$$\frac{M_m}{\rho_m} + \frac{M_r}{\rho_r} = \frac{1}{\rho_{th}} \quad (1)$$

*Experimental density by Archimedes principle*: Experimental/actual density ( $\rho_c$ ) of each test specimen (Table 3) are calculated using equation (2) and the average of these densities is used to determine wear loss of the composite. Density ( $\rho_w$ ) of tap water is considered as 1g/cc.  $M$  and  $M_w$  are the masses in air and water respectively.

$$\rho_c = \frac{M}{M - M_w} \times \rho_w \quad (2)$$

Table 3

Experimental density of the developed composite

Sample No.	Mass of the composite in air, $M$ (gm)	Mass of the composite in water, $M_w$ (gm)	Density of water, $\rho_w$ (g/cc)	Experimental Density, $\rho_c$ (g/cc)	Average experimental density (g/cc)
1	5.19	3.35	1	2.821	2.809
2	5.23	3.39	1	2.842	
3	5.22	3.38	1	2.837	
4	5.43	3.43	1	2.715	
5	5.06	3.27	1	2.827	
6	5.13	3.29	1	2.788	
7	4.97	3.19	1	2.792	
8	4.95	3.19	1	2.813	
9	4.3	2.79	1	2.848	

### 2.3 Porosity

Porosity of composite indicates its compactness. Less percentage porosity means less void space in the specimen and it indicates defect free, void less and successful fabrication of the composite. Average porosity of the composite is calculated (equation 3) as 1.672% as given in Table 4.

$$\% \text{ Porosity} = \frac{\text{Theoretical density} - \text{Actual density}}{\text{Theoretical density}} \times 100\% \quad (3)$$

Table 4

Porosity in the test samples prepared from the developed composite

Sample No.	Theoretical density, $\rho_{th}$ (g/cc)	Experimental/actual density, $\rho_c$ (g/cc)	Porosity (%)	Average porosity (%)
1	2.857	2.821	1.260	1.672
2	2.857	2.842	0.525	
3	2.857	2.837	0.700	
4	2.857	2.715	4.970	
5	2.857	2.827	1.050	
6	2.857	2.788	2.415	
7	2.857	2.792	2.275	
8	2.857	2.813	1.540	
9	2.857	2.848	0.315	

### 2.4 Hardness

Vicker microhardness tests (applied load 200 gf, dwell time 10 sec) of prepared composite are performed as per ASTM E384-22 standard [19] using the digital Vickers micro hardness tester machine (Fig. 2a). The Fig. 2b shows a square-based pyramidal-shaped diamond indenter with face angles of  $136^\circ$  and one of its indentations on surface of test sample is shown in Fig. 2c.

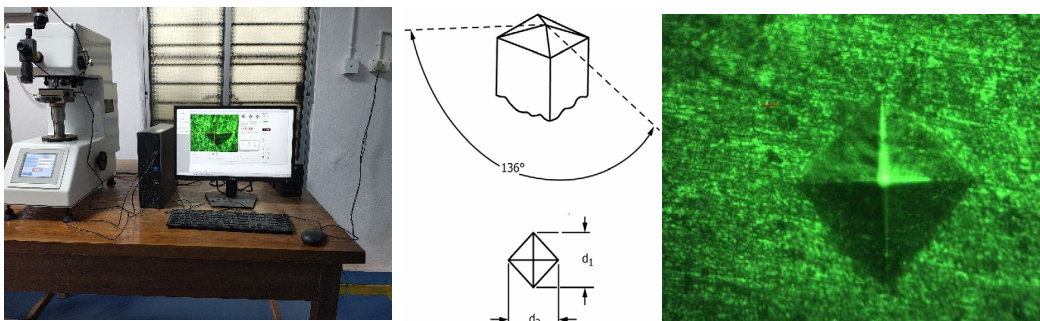


Fig. 2. Hardness measurement (a) digital Vickers microhardness machine (b) Vickers indenter, and (c) indentation on surface of test sample.

In this test, hardness is calculated using equation (4) [19] and the test is repeated six times (Table 5). The average Vickers microhardness of the prepared composite is 113.13 HV0.2. Hardness is measured in all the 9 types of specimens at six different positions on their centre lines and the consistent value is considered in each type. The variation in hardness of those specimens is noticed less than 3%. Hardness of the specimen number 8 whose porosity (1.540) is very close to the average porosity (1.672), is shown in Table 5 at all the six positions on the centre line.

$$HV = 1854.4 \times \frac{P}{d^2} \tag{4}$$

Where,  $P$  = Force, gf,  $d$  = Mean diagonal length of the indentation,  $\mu\text{m}$ .

Table 5

Average value of Vickers microhardness

Test No.	d1 ( $\mu\text{m}$ )	d2 ( $\mu\text{m}$ )	Mean dia. ( $\mu\text{m}$ )	Load (gm)	Dwell time (sec)	Hardness (HV)
1	57.01	59.6	58.31	200	10	109.10
2	58.08	59.45	58.77	200	10	107.40
3	53.66	51.22	52.44	200	10	134.87
4	56.4	58.54	57.47	200	10	112.29
5	62.5	63.11	62.81	200	10	94.03
6	56.4	54.27	55.34	200	10	121.12
Average (HV):						113.13

### 2.5 EDX Analysis

EDX analysis of sample having 4mm height and 10 mm diameter is carried out using FESEM. The EDX spectrum with atomic and weight percentages of elements confirm the presence of tungsten carbide (WC) within the composites (Fig. 3).

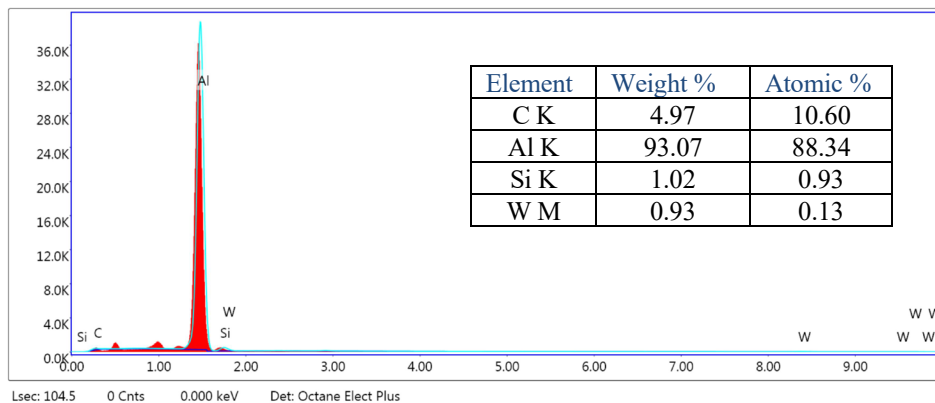


Fig. 3. EDX spectrum of Al7075/WC composite.

## 2.6 Wear Tests

Specimens (diameter: 10 mm, height: 22 mm) for wear tests (ASTM G99-95 standard) [20] are prepared from the composite by CNC Lath machine (machining operation) and CNC wire cut EDM machine (cutting operation), as shown in Fig. 4a with the help of a clamping device (Fig. 4b). Different grid sizes (1000, 1200, 1500 and 2000) of silicon carbide emery paper are used for finishing and flatness of specimen surfaces with the help of a specimen holder (Fig. 4c). Then, acetone (Fig. 4d) is used to clean the pin and disc. Now, specimens are polished again by double disc polishing machine with the help of polishing cloths (1 micron) and diamond paste of 1 micron as shown in Fig. 4e. After polishing, the cleaned pin by acetone is dried and weighed using a high accuracy (0.0001g) digital electronic balance machine (Fig. 4f). Then specimen is fitted on Ducom manufactured pin-on-disc machine (disc material: EN31, speed: 60-2000 rpm, surface roughness: 1.6 Ra) at track radius 50mm under different operating parameters. The wear parameters considered for the experiments are given in Table 6.

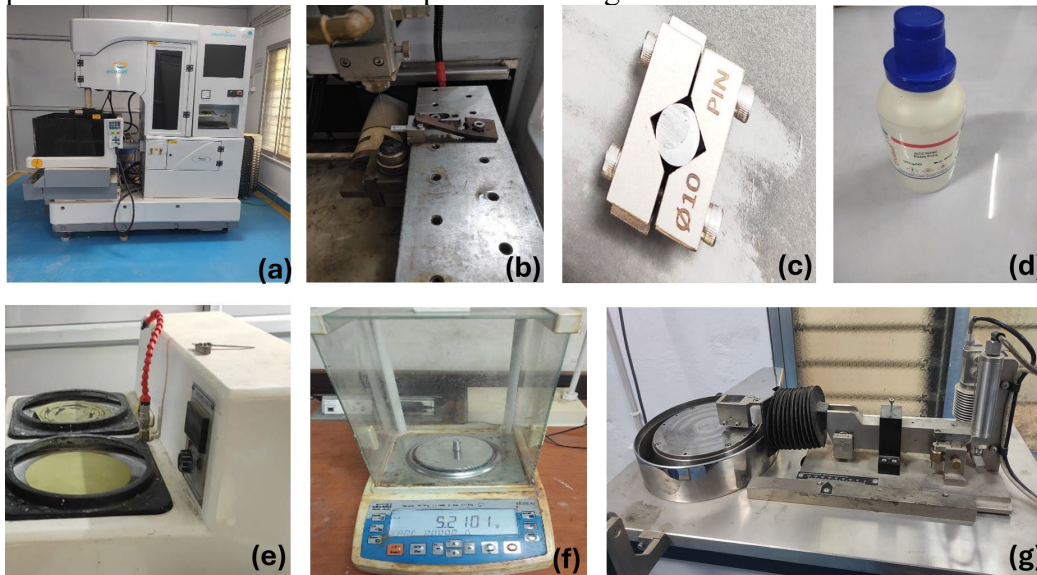


Fig. 4. Wear tests (a) CNC wire cut EDM machine (b) clamping of specimen for cutting from EDM machine (c) tool holder for grinding (d) acetone (e) double disc polishing (f) digital electronic weighing balance and (g) Pin-on-Disc machine.

Tested specimens are cleaned again with acetone and re-weighed in the same balancing machine. The wear loss is the mass loss of the original specimen after conducting wear tests. Volume loss is determined by dividing the mass loss by average experimental density. Variation of friction coefficient is also recorded during the wear tests. Experimental setup for wear tests is shown in Fig. 4g.

### 3. Results and Discussion

#### 3.1 Taguchi DOE analysis

Properties of the composite obtained from the wear tests following Taguchi L-9 orthogonal array [21,22] is given in Table 6. Influence of the control parameters on the wear behaviour of the composite is determined by using S/N (signal-to-noise) response analysis. Response variable of Table 7 is the wear loss. The ‘smaller-the-better’ condition is selected to analyse the wear behaviour of the AA7075/WC composite. The signal-to-noise (S/N) ratio for ‘smaller-is-better’ was calculated directly from MINITAB statistical software by using the formula as equation (5);

$$\text{S/N Ratio} = -10 \log [1/n (\Sigma y^2)] \quad (5)$$

Where, y is the observed data (wear) and n is the number of observations.

Table 6

Taguchi L-9 Orthogonal array with wear properties

Levels	Sliding Distance (m)	Applied Load (N)	Sliding Speed (m/s)	Initial weight (gram)	Final weight (gram)	Wear (gram)	Wear (cc)	Coefficient of friction (average)	S/N Ratio (wear)
1	500	20	1	5.1415	5.1388	0.0027	0.000961	0.281	60.3442
2	500	30	2	5.2101	5.2077	0.0024	0.000854	0.298	61.3672
3	500	40	3	5.1539	5.1511	0.0028	0.000997	0.332	60.0283
4	1000	20	2	5.398	5.3947	0.0033	0.001175	0.293	58.6012
5	1000	30	3	5.027	5.0211	0.0059	0.002100	0.347	53.5544
6	1000	40	1	5.1152	5.0992	0.016	0.005696	0.325	44.8890
7	1500	20	3	5.0051	4.9879	0.0172	0.006123	0.354	44.2609
8	1500	30	1	4.9197	4.8993	0.0204	0.007262	0.312	42.7788
9	1500	40	2	4.2994	4.2765	0.0229	0.008152	0.277	41.7747

Responses for S/N ratios and data means are shown in Table 7 which is obtained from Table 6 for different levels. The absolute difference (Delta) is the difference of their maximum and minimum values. As the sliding distance has the higher value of Delta (rank 1), this is a dominant factor on the wear. The influence of control factors, sliding distance, applied load and sliding speed on wear are graphically (main effect plots) represented in Fig. 5 based on the mean of S/N ratios and mean of means using MINITAB software. It can be observed that the main effect plot curve is steeper for sliding distance indicating more influential control factor on wear.

Table 7

## Responses for signal-to-noise ratios and data means

Response for Signal to Noise (S/N) Ratios				Response for Means			
Levels	Sliding Distance (m)	Load (N)	Sliding Speed (m/s)	Levels	Sliding Distance (m)	Load (N)	Sliding Speed (m/s)
1	60.58	54.40	49.34	1	0.000937	0.002753	0.004640
2	52.35	52.57	53.91	2	0.002990	0.003406	0.003394
3	42.94	48.90	52.61	3	0.007179	0.004948	0.003073
Delta	17.64	5.50	4.58	Delta	0.006242	0.002195	0.001566
Rank	1	2	3	Rank	1	2	3

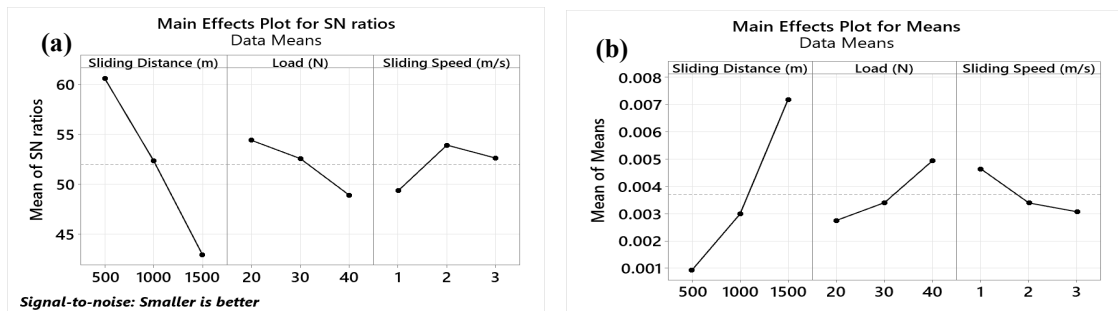


Fig. 5. Main effect plots for (a) S/N ratios and (b) means

## 3.2 Analysis of Variance

The percentage contribution of the control factors during wear process is determined by Analysis of Variance known as ANOVA (confidence level 95%) using MINITAB software (Table 8). It is found that the sliding distance has the highest influence (78.75%) on wear followed by applied load (9.74 %) and sliding speed (4.96%).

Table 8

## Analysis of Variance for data means

Source	DF	Seq SS	Contribution	Adj SS	Adj MS	F-Value	P-Value
Regression	3	0.000069	93.45%	0.000069	0.000023	23.78	0.002
Sliding Distance (m)	1	0.000058	78.75%	0.000058	0.000058	60.12	0.001
Load (N)	1	0.000007	9.74%	0.000007	0.000007	7.44	0.041
Sliding Speed (m/s)	1	0.000004	4.96%	0.000004	0.000004	3.79	0.109
Error	5	0.000005	6.55%	0.000005	0.000001		
Total	8	0.000074	100.00%				

DF: Degree of freedom, Seq SS: Sequential Sum of squares, Adj SS: Adjusted sum of squares, Adj MS: Adjusted mean squares, F-value = Adj MS for the factor/ Adj MS for the error.

The degree of freedom (DF) for regression in ANOVA table is equal to the number of independent variables (sliding distance, load, sliding speed) in the model i.e., 3. The F-value is a test statistic used in statistical tests and the P-value is the probability used in hypothesis testing.

### 3.3 Analysis of Coefficient of friction

The variation of coefficient of friction (COF) with respect to time at different wear conditions is shown in Fig. 6. Fluctuating line represents the instantaneous coefficient of friction which can be measured at any point corresponding to time during the wear test of prepared composite.

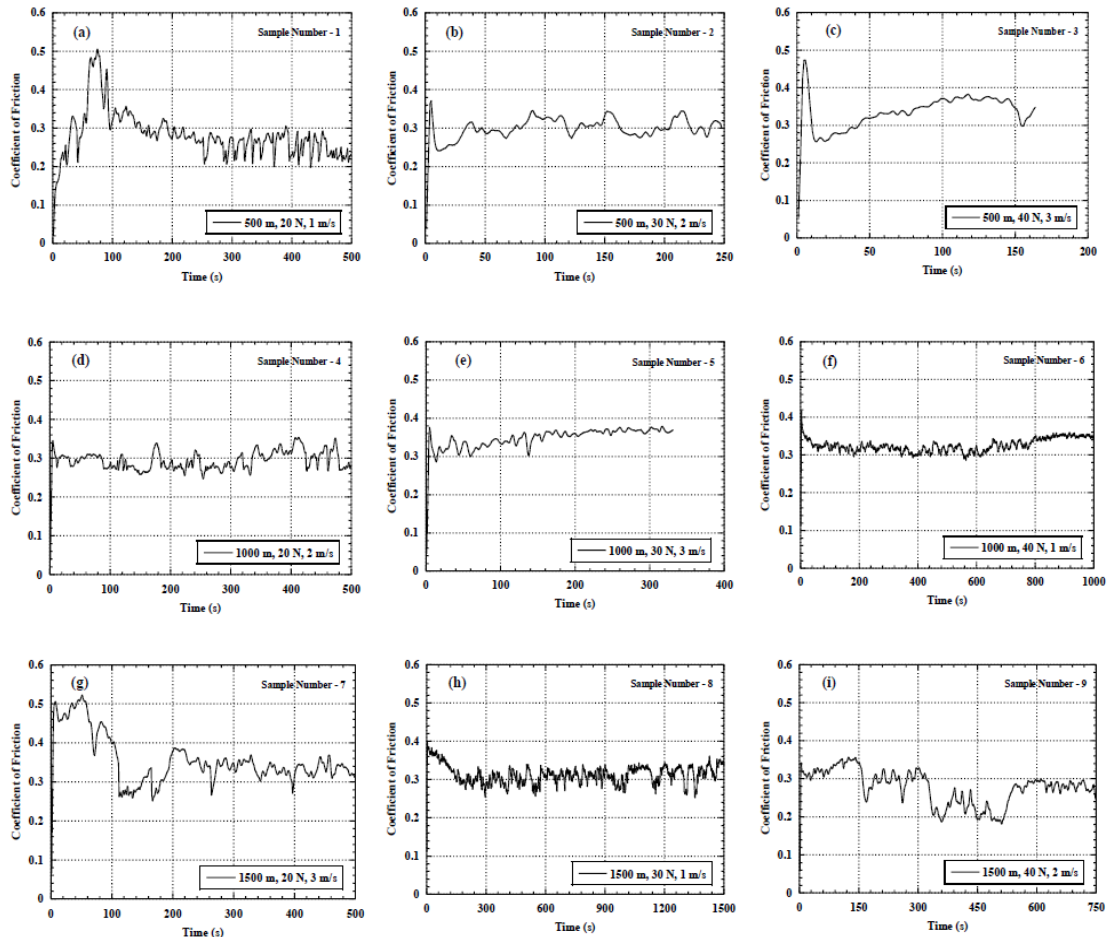


Fig. 6. Variation in COF with respect to time for different controlling factors.

The average coefficient of friction of the entire test, gives an overall idea of the frictional behaviour of the material under the different wear parameters. The coefficient of friction starts at a relatively higher value and then rapidly decreases and fluctuates significantly around the mean value of COF and settles into a more or less steady state, as shown in Figs. 6 (a-i). The fluctuations suggest that the friction is not constant and is likely influenced by factors such as the generation of wear debris, micro pit, micro crack, scratches, grooves and ploughing and potential slight variations in the testing conditions. Dynamic nature of friction was observed during wear. The average COF at different wear parameters is given in Table 6. The COF is high at condition, 1500 m, 20 N and 3 m/s. On increasing applied load (20-40 N) and sliding speed (1-3 m/s), the friction coefficient (COF) increases at sliding distance 500 m. At sliding distance 1500 m, the friction coefficient decreased considerably on increasing applied load (30-40 N) and sliding speed (1-2 m/s) as shown in Table 6. At high sliding speed, both the counter surfaces find less time for area of contact, resulting a low value of COF. The COF value at 1000 m, increases on increasing the applied load (20-30 N) and the sliding speed (2-3 m/s), whereas, decreases with increasing applied load (30-40 N) and decreasing sliding speed (3-1 m/s), as shown in Table 6. The COF increases during the initial period of the wear test due to changes in the contact surfaces, such as the formation of wear debris or the breakdown of surface layers. Once the surfaces stabilize and a steady-state condition is reached, the COF fluctuates. The smooth surfaces become rougher as wear progresses based on the applied conditions. The increased roughness leads to greater mechanical interlocking and a higher COF as in Figs. 6 (c) and (e). As per the conditions, Figs. 6 (c) and (e) falls under shorter time duration. Also, the accumulation and compaction of wear debris in the contact zone, increases the surface roughness and resistance to sliding, therefore, those graphs are increasing continuously [23]. Now, each graph indicates the sample number, as suggested by the reviewer. There were no pores on the contact surfaces of the samples as the contact surfaces were finished by emery papers and polished by double disc polishing machine before the wear tests.

### *3.4 Worn-out surfaces analysis*

After conducting wear tests, the worn-out surfaces of AA7075/WC specimens as shown in images (magnification 200x) of Figs. 7 (a-i), are analysed for different controlling parameters using optical microscope. The micro pit, micro crack, scratches and grooves contribute to the significant wear loss of the prepared composites.

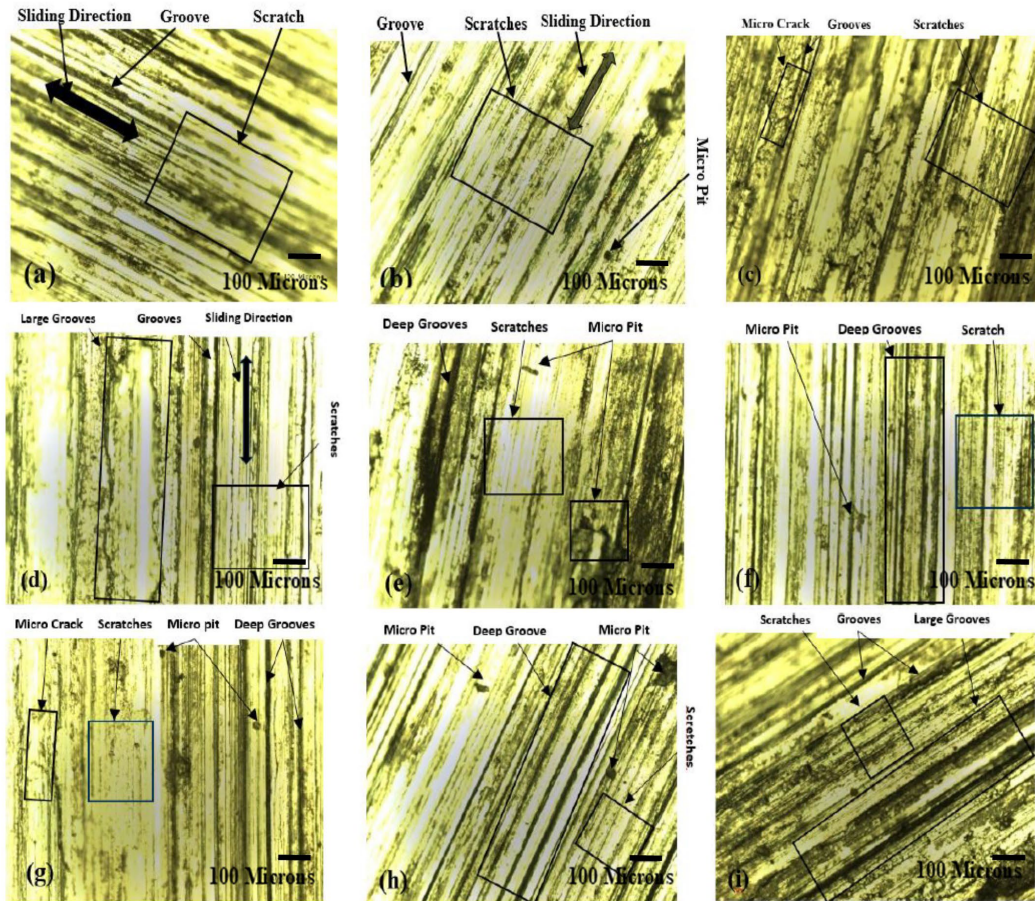


Fig. 7. Worn-out surfaces for wear condition (a) 500 m, 20 N, 1 m/s (b) 500 m, 30 N, 2 m/s (c) 500 m, 40 N, 3 m/s (d) 1000 m, 20 N, 2 m/s (e) 1000 m, 30 N, 3 m/s (f) 1000 m, 40 N, 1 m/s (g) 1500 m, 20 N, 3 m/s (h) 1500 m, 30 N, 1 m/s; and (i) 1500 m, 40 N, 2 m/s.

The smaller wear grooves, no micro crack and no micro pitting are observed along the sliding direction, which contributes to a lower wear loss at 500 m sliding distance, 20 N load and 1 m/s sliding speed, as shown in Fig. 7 (a), scale of 100 microns is indicated with each image. Deeper and wider scratches on the surface are observed as wear grooves. The worn-out surface has larger wear grooves (parallel scratches) for 1000 m sliding distance, 40 N applied load and 2 m/s sliding speed, indicating high surface wear, Fig. 7 (i). More scratches and grooves are observed on worn-out surface which shows the characteristics of abrasive wear. The grooves are aligned with the sliding direction which indicates abrasive wear as shown in Figs. 7 (a-i).

#### 4. Conclusions

In this paper, the aluminium matrix composite AA7075/WC is developed using stir casting method and effects of control parameters (sliding distance, applied load and sliding speed) on the wear properties of the composite are studied. Thereafter, these parameters are optimized using the well-known Taguchi method.

Following are the important findings of the present investigation:

- The wear on the prepared composite AA7075/2 wt.% WC is influenced greatly by the sliding distance (78.75%) followed by applied load (9.74 %) and sliding speed (4.96%).
- The highest coefficient of friction (COF) is obtained at 1500 m sliding distance, 20 N applied load and 3 m/s sliding speed, whereas, the lowest COF is obtained at 1500 m sliding distance, 40 N applied load and 2 m/s sliding speed. On increasing applied load (20-40 N) and sliding speed (1-3 m/s), the COF increases for sliding distance 500 m.
- At sliding distance 1500 m, the COF decreases when applied load (30-40 N) and sliding speed (1-2 m/s) increase.
- The micro pit, micro crack, scratches and grooves phenomena contribute to significant wear loss of prepared composites. More scratches and grooves on the worn-out surface show the characteristics of abrasive wear.
- It was observed that the average Vickers microhardness of prepared aluminium matrix composite (AA7075/2 wt.% WC) is 113.13 HV0.2.
- Less percentage porosity (1.672%) indicates the defect free and successful preparation of the composite.

#### REFERENCES

- [1] *N. Valizade, Z. Farhat*, "A Review on Abrasive Wear of Aluminum Composites: Mechanisms and Influencing Factors", *J. Compos. Sci.*, 8, 2024, 149.
- [2] *K. Jayappa, K. C. Anil, Z. A. Khan*, "Enhancing wear resistance in Al-7075 composites through conventional mixing and casting techniques", *Journal of Materials Research and Technology*, 27, 2023, 7935-7945.
- [3] *D. Tana, S. Xia, A. Yob, K. Yang, S. Yan, M. Givord, D. Liang*, "Evaluation of the wear resistance of aluminium-based hybrid composite brake discs under relevant city rail environments", *Materials & Design*, 215, 2022, 110504.
- [4] *K. Sharma, R. Bhandari, A. Aherwar, R. Rimašauskiene, C. Pinca-Bretotean*, "A study of advancement in application opportunities of aluminum metal matrix composites", *Materials Today: Proceedings*, 26, 2020, 2419-2424.
- [5] *K. Prakash, N. K. Singh*, "Optimum Composition of Aluminium Hybrid Composites for Maximum Wear Resistance", *Solid State Phenomena*, 319, 2021, 18-23.
- [6] *S. Ahmad, Y. Tian, A. W. Hashmia, R. K. Singh, F. Iqbal, S. Dangi, A. Alansari, C. Prakash, C. K. Chan*, "Experimental studies on mechanical properties of Al-7075/TiO<sub>2</sub>

- metal matrix composite and its tribological behaviour”, *Journal of Materials Research and Technology*, 30, 2024, 8539–8552.
- [7] K. J. “Investigating run-in and steady-state wear mechanisms of Al-7075 alloy hybrid composite for brake rotor applications”, *Results in Surfaces and Interfaces*, 16, 2024, 100280.
- [8] O. Aranke, C. Gandhi, N. Dixit, P. Kuppan, “Influence of Multiwall Carbon Nanotubes (MWCNT) on Wear and Coefficient of Friction of Aluminium (Al 7075) Metal Matrix Composite”, *Materials Today: Proceedings*, 5, 2018, 7748-7757.
- [9] Baradeswaran, A. E. Perumal, “Influence of B4C on the tribological and mechanical properties of Al 7075–B4C composites”, *Composites: Part B*, 54, 2013, 146–152.
- [10] Baradeswaran, A. Elayaperumal, R. F. Issac, “A Statistical Analysis of Optimization of Wear Behaviour of Al Al<sub>2</sub>O<sub>3</sub> Composites Using Taguchi Technique”, *Procedia Engineering*, 64, 2013, 973-982.
- [11] N. Senthilkumar, K. Gajalakshmi, K. Palanikumar, B. Deepanraj, A. R. Afzal, “Wear analysis and optimization of nanoclay and copper coated carbon fiber strengthened hybrid aluminium composite”, *Results in Engineering*, 25, 2025, 103711.
- [12] P. B. Asha, S. S. Murthy, C. R. P. Rao, V. R. Kumar, R. Kiran, C. N. Suresha, “Optimization of Wear Factors of Aluminium Hybrid Metal Matrix Composites Using Taguchi Method”, *Journal of Minerals and Materials Characterization and Engineering*, 9, 2021, 38-47.
- [13] R. S. Rana, R. Purohit, A. K. Sharma, S. Rana, “Optimization of Wear Performance of AA 5083/10 wt.% SiCp Composites Using Taguchi Method”, *Procedia Materials Science*, 6, 2014, 503 – 511.
- [14] J. U. Prakash, A. D. Sadhana, S. Ananth, K. V.A. Pillai, “Optimization of wear parameters of aluminium matrix composites (LM6/Fly Ash) using Taguchi technique”, *Materials Today: Proceedings*, 39 (4), 2021, 1543-1548.
- [15] G. R. Gurunagendra, K. S. A. Kumar, V. Ravikumar, H. Yaragudri, R. S. Kumar, C. D. Prasad, C. Solaimuthu, A. Tiwari, S. R. Prabhu, “Application of the Taguchi technique to examine the wear patterns of zircon flour reinforcement in stir-cast zinc aluminium composites”, *Results in Surfaces and Interfaces*, 20, 2025, 100598.
- [16] P. Pasupulla, P. Amornphimoltham, P. Charles, V. S. Sundaram, M. M. Ramakrishna, “Taguchi L16 orthogonal array analysis on wear rate parameters for aluminum related hybrid composites”, *Materials Today: Proceedings*, 62 (4), 2022, 1692-1696.
- [17] S. Deepak, H. S. Balasubramanya, H. L. Nandeesh, G. B. V. Kumar, A. S. D. Shetty, “Tribological Behaviour of Aluminium/WC Metal Matrix Composite Using ANN”, *JNNCE Journal of Engineering & Management*, 6 (1), 2022, 19-24.
- [18] Wang, Y. Sun, N. Wei, Y. Xu, L. Huang, “Microstructure and properties of Nano-WC particle-reinforced lamellar eutectic high-entropy S alloy by laser directed energy deposition”, *Intermetallics*, 188, 2026, 109038.
- [19] ASTM E384-22, “Standard Test Method for Microindentation Hardness of Materials”, 2022.
- [20] ASTM G99-17, “Standard Test Method for Wear Testing with a Pin-on-Disk Apparatus”, 2023.
- [21] V. Mohanvel, S. Prasath, K. Yoganandam, B.G. Tesemna, S.S. Kumar, “Optimization of Wear parameters of aluminium composites (AA7150/10 wt %WC) employing Taguchi approach”, *Materials Today: Proceedings*, 33 (7), 2020, 4742-4745.

- [22] *Stojanovic, J. Blagojevic, M. Babic, S. Velickovic, S. Miladinovi*, “Optimization of hybrid aluminum composites wear using Taguchi method and artificial neural network”, *Industrial Lubrication and Tribology*, 69 (6), 2017, 1005-1015.
- [23] *N. Valizade, Z. Farhat*, “A Review on Abrasive Wear of Aluminum Composites: Mechanisms and Influencing Factors”, *J. Compos. Sci.*, 8 (4), 2024, 149, <https://doi.org/10.3390/jcs8040149>.